

See discussions, stats, and author profiles for this publication at: <https://www.researchgate.net/publication/259988235>

Linear control of the flywheel inverted pendulum

Article in *ISA Transactions* · September 2014

DOI: 10.1016/j.isatra.2013.12.030 · Source: PubMed

CITATIONS

18

READS

641

2 authors:



Manuel Olivares

Universidad Técnica Federico Santa María

49 PUBLICATIONS 137 CITATIONS

[SEE PROFILE](#)



P. Albertos

Universitat Politècnica de València

354 PUBLICATIONS 2,460 CITATIONS

[SEE PROFILE](#)

Some of the authors of this publication are also working on these related projects:



Profesion@l: Equilibrio de género en el espacio europeo [View project](#)



DGIP 23.15.26 - Control de un manipulador robótico continuo [View project](#)

Linear control of the flywheel inverted pendulum

Manuel Olivares^a, Pedro Albertos^{b,*}

^a*Departamento de Electrónica, Universidad Técnica Federico Santa María, Valparaíso, Chile*

^b*Instituto de Automática e Informática Industrial, Universitat Politècnica de València, València 46022, Spain*

Abstract

The flywheel inverted pendulum is an underactuated mechanical system with a nonlinear model but admitting a linear approximation around the unstable equilibrium point in the upper position. Although underactuated systems usually require nonlinear controllers, the easy tuning and understanding of linear controllers make them more attractive for designers and final users. In a recent paper, a simple PID controller was proposed by the authors, leading to an internally unstable controlled plant. To achieve global stability, two options are here developed: first by introducing an internal stabilizing controller and second by replacing the PID controller by an observer-based state feedback control. Simulation and experimental results show the effectiveness of the design.

Keywords: Inverted pendulum, underactuated systems, PID control design, internal instability

1. Introduction

Underactuated mechanical systems received a lot of interest as they appear in many practical applications such as robotics systems (e.g. mobile robots, flexible-link robots, snake-type robots, walking robots), aerospace systems (e.g. aircraft, spacecraft, helicopters, rockets and satellites), or marine vehicles (e.g. surface vessels and underwater vehicles). They are characterized by the fact that there are more degrees of freedom than actuators, i.e., one or more degrees of freedom are unactuated [1] presenting challenging control problems to solve operational inconveniences with great interest from theoretical point of view. Most of the reported works on this kind of mechanical systems approach the problem from a nonlinear perspective [2], [3], [4], [5]. The linear approximation around equilibrium points may not, in general, be controllable and the feedback stabilization approach to transform the plant into a linear one, in general, can not be used. Therefore linear control methods are not used to solve the feedback stabilization problem, not even locally. In the same way, the tracking control problem can not be transformed into a linear control problem.

But linear control systems are very appealing by their simplicity and easy tuning. The design procedure may have different steps in order to consider different situations but, in any case, a clear understanding of the design parameters is at hand. With this idea in mind, in our previous paper, [6], a PID controller was proposed to control a flywheel inverted pendulum (FIP) [7]. Due to the under-actuation, a derivative behavior appears at the plant output, so the upper equilibrium position can be reached for any constant or null input value, if the overall system is stable. The problem already reported is that the PID solution is internally unstable.

The paper is organized as follows. First, to fix the problem, the nonlinear model and its approximated linearization around the unstable equilibrium point for this well-known mechanical device are derived. Then, the design of a PID controller to stabilize the plant and to compensate measurement disturbances is reviewed. Looking at the FIP model, it presents an unstable open-loop pole and a zero at the origin. So, even though the input/output behavior of the controlled plant appears to be stable, its internal stability is not achieved. To stabilize the internally unstable controlled plant, two options are considered: first a new control loop is added, keeping the global stability achieved by the initial design and allowing to control the unstable internal variable. The second option is a state feedback control, where cancelation is avoided. This results in a good behavior but it requires full access to the state, thus a state estimator/observer should be implemented. These results are illustrated experimentally by the control of a laboratory prototype. Some comments and future works are outlined in the last section, where the improvements with respect to the previous paper are discussed.

2. Flywheel Inverted Pendulum

A review on the control of underactuated systems can be found in [1] and [8] (where the classical inverted pendulum mounted on a cart is used as a benchmark of underactuated system), as well as in [9], [10], where controllers have been designed by using linearization-based or energy-based methods.

Among the different approaches to control the FIP, a swinging-up control at the unstable equilibrium point, without flywheel angular velocity control, has been reported [11], [12], a fuzzy control is reported in [13] and a linear full space state control design using pole assignment has been deeply studied in [14]. As already mentioned, a PID simple solution was proposed in [6].

*Corresponding author. Tel. +34(96)3879570

Email addresses: manuel.olivares@usm.cl (Manuel Olivares), pedro@aii.upv.es (Pedro Albertos)

2.1. The model

A FIP consists of an inverted pendulum pivoting on a frictionless point with a rotating mass on the top. It is an abstraction of a biped robot, with an articulated/motorized joint, where the leg is represented by a bar and the moving body is abstracted as a rotating motor. The reaction torque generated by this rotation allows moving forward/backward the upper part of the pendulum. A local sensor placed at the bottom of the pendulum provides a measurement of its inclination. A picture of such a device [7] is shown in Fig. 1(a) and a schematic diagram of the pendulum is depicted in Fig. 1(b).

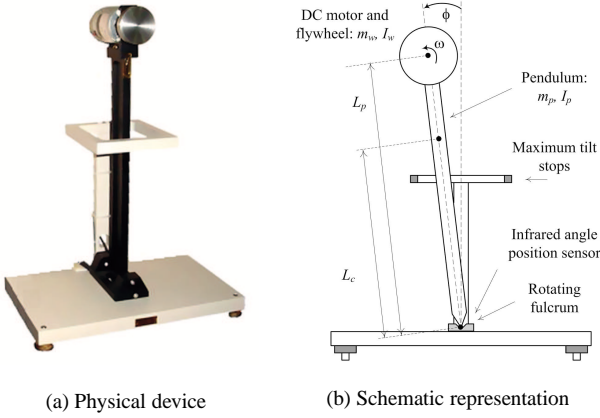


Figure 1: Flywheel Inverted Pendulum

A DC motor controlled by the armature voltage is moving the inertia wheel. The main parameters to be considered are the armature resistance (R) and inductance (L), as well as the torque constant (M).

2.1.1. Lagrangian formulation

Define by $\{m_p, I_p, \phi\}$ the pendulum mass, its moment of inertia with respect to the base and its angular position with respect to the vertical axis, respectively; and by $\{m_w, I_w, \theta\}$ the flywheel mass, its moment of inertia with respect to its center of mass and its rotation angle, respectively.

The Lagrangian is defined by (1), where E , V denote the kinetic and potential energies, respectively, and q is the generalized coordinates vector of the system, $q = [\phi \quad \theta]^T$.

$$L(q, \dot{q}) = E(q, \dot{q}) - V(q, \dot{q}) \quad (1)$$

The system dynamics is derived from the Euler-Lagrange equation (2), where R is the Rayleigh's dissipative function and τ_i are the moments applied to each coordinate (pendulum bar and flywheel).

$$\frac{d}{dt} \left(\frac{\partial L}{\partial \dot{q}_i} \right) - \frac{\partial L}{\partial q_i} + \frac{\partial R}{\partial \dot{q}_i} = \tau_i; \quad i = \phi, \theta \quad (2)$$

The total kinetic energy can be easily expressed as

$$E(q, \dot{q}) = \frac{1}{2} [I_p \dot{\phi}^2 + I_w \dot{\theta}^2 + m_w L_p^2 \dot{\phi}^2] \quad (3)$$

where I_p and I_w are the inertia moments of the pendulum bar with respect to the fulcrum and the flywheel with respect to its rotation axis, respectively, and L_p is the pendulum length (from the flywheel axis to the fulcrum).

The potential energy is given by

$$V(q, \dot{q}) = m_p g L_c \cos \phi + m_w g L_p \cos \phi \quad (4)$$

where L_c is the pendulum mass center distance to the fulcrum.

Thence, altogether, the Lagrangian is given by

$$\begin{aligned} L(q, \dot{q}) &= \frac{1}{2} \alpha_1 \dot{\phi}^2 + \frac{1}{2} I_w \dot{\theta}^2 - \alpha_2 \cos \phi \\ \alpha_1 &= m_w L_p^2 + I_p \\ \alpha_2 &= (m_p L_c + m_w L_p) g \end{aligned} \quad (5)$$

If (2) is applied, taking into account that the generalized moment of the system and the dissipative moments are given by (6), where η_ϕ and η_θ are friction factors and τ is the external torque applied to the flywheel,

$$\begin{aligned} \tau_\phi &= -I_w \ddot{\theta}; & \frac{\partial R}{\partial \dot{\phi}} &= \eta_\phi \dot{\phi} \\ \tau_\theta &= \tau - I_w \ddot{\phi}; & \frac{\partial R}{\partial \dot{\theta}} &= \eta_\theta \dot{\theta} \end{aligned} \quad (6)$$

then the nonlinear model of the FIP is expressed by the coupled equations

$$\alpha_1 \ddot{\phi} + I_w \ddot{\theta} = \alpha_2 \sin \phi - \eta_\phi \dot{\phi} \quad (7)$$

$$I_w (\ddot{\phi} + \ddot{\theta}) = \tau - \eta_\theta \dot{\theta} \quad (8)$$

The input torque $\tau = M i_a$ generated by the electric motor, where i_a is the armature current, is obtained from the differential equation of the armature electric circuit

$$v_a = R_a i_a + L_a \frac{di_a}{dt} + v_r \quad (9)$$

Note that $v_r = M \dot{\theta}$ is the e.m.f. and v_a , the armature voltage, is the externally manipulated variable.

2.2. Linearized Model

To analyze the dynamic behavior of the FIP around the unstable upper position equilibrium point ($\phi_0 = 0$), the above model equations are linearized. It is worth noting that only (7) is nonlinear and easy to linearize, leading to the following equations

$$\alpha_1 \ddot{\phi} + I_w \ddot{\theta} = \alpha_2 \phi - \eta_\phi \dot{\phi} \quad (10)$$

$$I_w (\ddot{\phi} + \ddot{\theta}) = M i_a - \eta_\theta \dot{\theta} \quad (11)$$

$$L_a \dot{i}_a + R_a i_a + M \dot{\theta} = v_a \quad (12)$$

The angular position ϕ is measured by means of an infrared sensor located at the bottom of the pendulum, providing a proportional voltage

$$v_\phi = K_m \phi \quad (13)$$

The DC motor armature voltage is obtained from a low power voltage input u by means of a power amplifier, given by

$$v_a = -K_a u \quad (14)$$

Assuming a state vector $x = [\phi \ \dot{\phi} \ \theta \ \dot{\theta} \ i_a]^T$, and considering the single control input u from (14) and the output $y = v_\phi$ given by (13), the state space representation is

$$\begin{aligned} \dot{x} &= \begin{bmatrix} 0 & 1 & 0 & 0 & 0 \\ \frac{\alpha_2}{\alpha_1 - I_w} & \frac{-\eta_\phi}{\alpha_1 - I_w} & 0 & \frac{\eta_\theta}{\alpha_1 - I_w} & \frac{-M}{\alpha_1 - I_w} \\ 0 & 0 & 0 & 1 & 0 \\ \frac{-\alpha_2}{\alpha_1 - I_w} & \frac{\eta_\phi}{\alpha_1 - I_w} & 0 & -\eta_\theta \beta & M\beta \\ 0 & 0 & 0 & \frac{-M}{L_a} & \frac{-R_a}{L_a} \end{bmatrix} x \\ &+ \begin{bmatrix} 0 \\ 0 \\ 0 \\ 0 \\ \frac{-K_a}{L_a} \end{bmatrix} u \\ y &= [K_m \ 0 \ 0 \ 0 \ 0] x \end{aligned} \quad (15)$$

where

$$\beta = \frac{1}{\alpha_1 - I_w} + \frac{1}{I_w} \quad (16)$$

Simplified model. A simplified model can be obtained if some parameters are considered negligible. In particular L_a , η_θ and η_ϕ can be neglected ($L_a = \eta_\theta = \eta_\phi = 0$). It also appears that the third variable $x_3 = \theta$, the flywheel angular position, does not affect any other variable (third column of the system matrix (15) is null). Thus, if there is not any interest on its evolution, it can be discarded.

Then, from (12), the armature current i_a can be obtained

$$i_a = \frac{-1}{R_a} (K_a u + M \dot{\theta}) \quad (17)$$

and the FIP can be represented by the third order model

$$\begin{aligned} \dot{z} &= \begin{bmatrix} 0 & 1 & 0 \\ \frac{\alpha_2}{\alpha_1} & 0 & \frac{M^2}{\alpha_1 R_a} \\ \frac{-\alpha_2}{\alpha_1} & 0 & -M\gamma \end{bmatrix} z + \begin{bmatrix} 0 \\ \frac{MK_a}{\alpha_1 R_a} \\ -K_a \gamma \end{bmatrix} u \\ y &= [K_m \ 0 \ 0] z \end{aligned} \quad (18)$$

where $z = [\phi \ \dot{\phi} \ \dot{\theta}]^T$ and

$$\gamma = \frac{M}{R_a} \left(\frac{1}{I_w} + \frac{1}{\alpha_1} \right) \quad (19)$$

In the next sections, the external input voltage $u(t)$, corresponding to the control input, the output voltage $v_\phi(t)$ corresponding to the pendulum angular position, and the unmeasured state $\omega(t) = \dot{\theta}(t)$ corresponding to the flywheel angular velocity are considered, although it seems obvious that only one variable can be controlled with one control action.

3. Experimental set-up and PID control

A laboratory prototype [7] is shown in Fig. 1(a). Since there are instrumentation constraints (only the pendulum angular position $\phi(t)$ is measured in this equipment) an output feedback controller is foreseen.

3.1. Numerical data

For this lab prototype, the FIP parameters are provided in Table 1.

Table 1: FIP Parameters

Symbol	Description	Value
m_p	Pendulum mass	0.3046[kg]
m_w	Motor and flywheel mass	0.2804[kg]
I_p	Pendulum inertial moment	0.043[kg · m ²]
I_w	Flywheel inertial moment	1.5 · 10 ⁻⁵ [kg · m ²]
L_p	Pendulum length	0.292[m]
L_c	Pendulum mass center	0.258[m]
M	Motor constant	0.0375[Nm/A]
R_a	Armature resistor	4.7[Ω]
K_a	Amplifier gain	1.1685[V/V]
K_m	Pendulum position sensor gain	107.47[V/rad]
g	Gravitational acceleration	9.8[m/s ²]

Thus equations (5) and (19) yield $\alpha_1 = 0.0669$, $\alpha_2 = 1.5725$ and $\gamma = 532.0341$, leading to the following state space representation

$$\begin{aligned} \dot{z} &= \begin{bmatrix} 0 & 1 & 0 \\ 23.5031 & 0 & 0.0045 \\ -23.5031 & 0 & -19.9513 \end{bmatrix} z \\ &+ \begin{bmatrix} 0 \\ 0.1393 \\ -621.6819 \end{bmatrix} u; \quad y = [107.47 \ 0 \ 0] z \end{aligned} \quad (20)$$

3.2. Model-based design

Let us consider the model derived above. From (20), the transfer function $G(s)$ is

$$G(s) = \frac{V_\phi(s)}{U(s)} = \frac{14.9751s}{(s + 19.95)(s + 4.847)(s - 4.848)} \quad (21)$$

showing three poles, one of them unstable, and one zero at the origin, considering $v_\phi(t)$ as the measured output variable and $u(t)$ the single control input. Due to the zero at the origin and the positive pole, the system is open loop unstable and non minimum phase.

The output feedback control loop to stabilize the pendulum in the upward position is represented in Fig. 2, where $\delta(t)$ is a measurement disturbance, initially assumed to be null, and the reference r_ϕ is zero corresponding to the upward pendulum position.

A basic PID controller $C_1(s)$ was proposed in [6] to stabilize the output, cancelling the fast stable plant pole and designing the closed loop polynomial $A_{cl}(s) = (s + \sigma)^2$ for $T(0) = 2$,

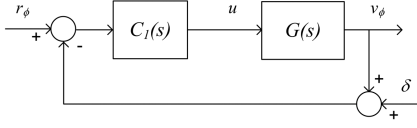


Figure 2: Output feedback FIP Control

yielding $K_{c1} = 16.1$, $T_{i1} = 0.26$ and $T_{d1} = 0.04$, leading to the input/output closed-loop transfer function (23).

$$C_1(s) = K_{c1} \left(1 + \frac{1}{T_{i1}s} + T_{d1}s \right) \quad (22)$$

$$T(s) = \frac{9.6951(s + 4.847)^2}{(s + 4.847)^3} \approx \frac{9.6951}{s + 4.847} \quad (23)$$

Note that $T(s)$ is stable, but $T(0)$ can not be designed to unity in steady-state even though the controller has an integrator, due to the controller-plant pole/zero cancellation.

The responses, using the simulated plant, are plotted in Fig. 3. Starting with the initial condition $v_\phi(0) = 0.2$, the output is stabilized and reaches the reference $r_\phi = 0$. A step measurement disturbance $\delta(t) = 0.2$ is applied at $t=1.5[s]$. The response is faster, reaching a steady-state error around $v_{\phi\infty} \approx -0.4$, but a constant flywheel angular acceleration, that is, a constant increment on the control signal is needed to compensate it leading to saturation. This control cannot be applied to the FIP as the control signal saturates at 10[V] (around 0.8[s] later), and with such a small measurement disturbance the pendulum falls down.

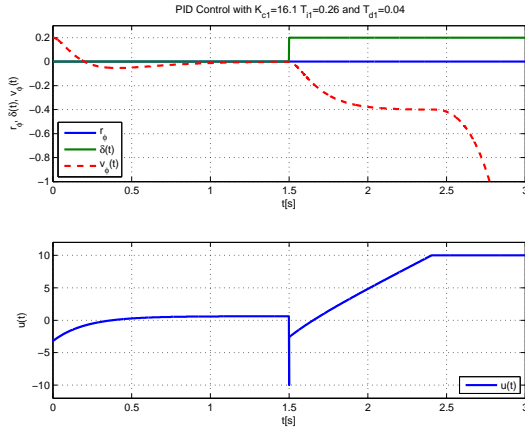


Figure 3: Simulated FIP with PID control: Time responses

Thence, as can be seen in the control sensitivity function $S_u(s) = \frac{U(s)}{R_\phi(s)}$ where an integrator appears, the controlled plant is internally unstable.

$$S_u(s) = \frac{C_1(s)}{1 + C_1(s)G(s)} \quad (24)$$

$$S_u(s) = \frac{0.64741(s + 19.95)(s + 4.847)^2(s - 4.848)}{s(s + 4.847)^2}$$

$$\approx \frac{0.64741(s + 19.95)(s - 4.848)}{s}$$

4. Internally stable design

The problem of the internal instability is due to the pole/zero cancellation at the origin. To avoid this cancellation, the PID controller can be modified, shifting the pole at the origin but in return the response will be slower. An alternative to remove the internal instability is by introducing an additional loop to control the plant input. This will also allow to determine the steady-state value of the wheel speed, required to balance the pendulum at the zero angular position. In this way, the saturation will not be reached.

The additional loop is conceived to stabilize and force the control action to be constant introducing a $r_\phi(t)$ pendulum position reference update to compensate measurement disturbances, with the control scheme shown in the block diagram of Fig. 4.

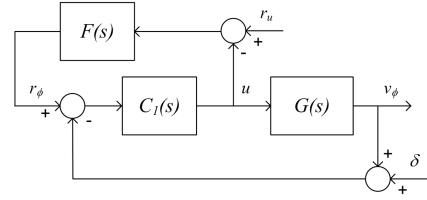


Figure 4: Internal instability outer loop compensator

The combined control loops are equivalent to the one shown in Fig. 5 that should be designed to keep the whole system stable, as the control sensitivity function (24) has embedded $C_1(s)$ and $G(s)$. In this case, a first order lag filter (25) has been designed to stabilize $S_u(s)$.

$$F(s) = \frac{K_f}{s + \alpha_f} \quad (25)$$

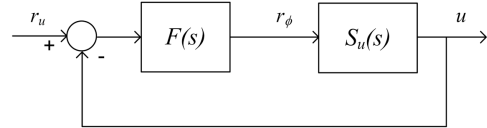


Figure 5: Control sensitivity function stabilization loop

The filter parameters $K_f = -1.24$ and $\alpha_f = 19.95$ are designed to get a stable closed loop polynomial $A_{cl}(s) = (s + \epsilon)^2$, for ϵ equal to the fast stable plant pole, giving the closed loop transfer function $H(s) = \frac{U(s)}{R_\phi(s)}$. Note that $H(s)$ is stable, non-minimum phase and has unitary static gain because of the $S_u(s)$ integrator.

$$H(s) = \frac{F(s)C_1(s)G(s)}{1 + C_1(s)(F(s) + G(s))}$$

$$= \frac{-4.1158(s + 19.95)^2(s + 4.847)(s - 4.848)}{(s + 19.95)^3(s + 4.847)^4} \quad (26)$$

$$\approx \frac{-4.1158(s - 4.848)}{s + 19.95}$$

The main advantage of the proposed design is the easy tuning and understanding of the parameters. Those of the PID are

selected to control the output. Those of $F(s)$ are determined to stabilize the system and as a slave controller sets the flywheel speed.

The system responses are plotted in Fig. 6. The response to an initial condition different from zero is very fast. The control action $u(t)$ is driven to the required initial zero reference $r_u(t) = 0$ at $t=1[s]$. The whole system is stable, although slower than before. Nevertheless, if there is a constant measurement disturbance $\delta(t) = 0.2$ at $t=1.5[s]$, the system output $v_\phi(t)$ now reaches the zero angular position with internal stability, as the reference $r_\phi(t)$ is updated by the filter, with steady-state error in the control action $u_\infty \approx 3.2$ for $r_u(t) = 0$. This error is compensated changing $r_u(t) = \frac{\delta}{F(0)}$ at $t=2.5[s]$, where $F(0) < 0$ is the static gain of the filter, setting r_u to stabilize the pendulum with minimum energy (zero flywheel angular velocity).

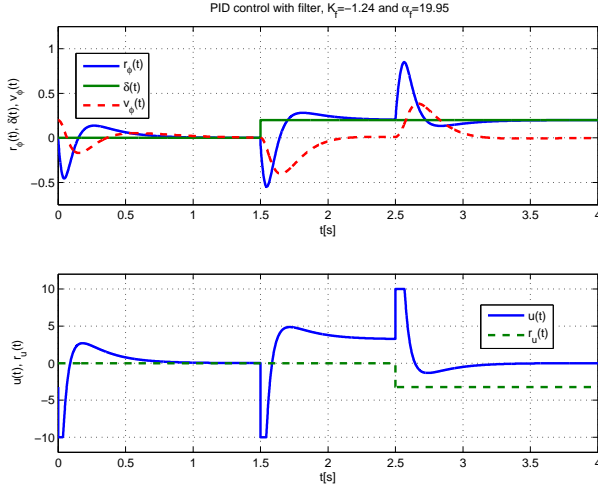


Figure 6: Measurement disturbance stable compensation

4.1. State feedback stabilizing controller

Another alternative, without the drawbacks of the PID control strategy shown in Fig. 3, is the use of a state feedback control designed to assign poles similar to those in (23). Assuming full access to the state space vector $z(t)$ of the simplified model (18), and using the numerical model (20), the state feedback control law $u = -K_{sf}x$ can be computed using LQR for $Q = I_{3 \times 3}$ and $R = 1000$ leading the state feedback vector gain $K_{sf} = [2.29 \cdot 10^3 \quad 4.72 \cdot 10^2 \quad 0.08]$. The state feedback control structure is shown in Fig. 7, and the ideal response is shown in Fig. 8.

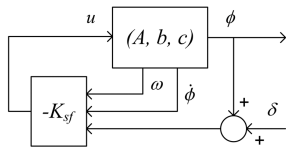


Figure 7: State Feedback Loop

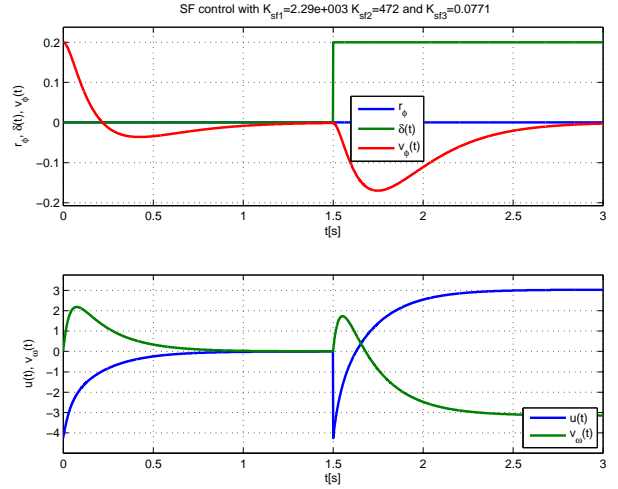


Figure 8: Ideal state feedback control: Time responses

In this case, the response is internally stable, but there is no control on the steady-state flywheel speed. Moreover, in general, the state vector is not fully accessible.

4.2. State-based output feedback stabilizing controller

As the only measurement is the pendulum position ϕ , the state space vector variables $\dot{\phi}$ and $\dot{\theta}$ should be estimated or computed. If a flywheel angular velocity sensor is available, with a gain $K_\omega = \frac{v_\omega}{\omega}$, only the output derivative should be computed. Then, a PD controller can be used.

The equivalent control structure is depicted in Fig. 9, where the controller $C_2(s)$ in (27) implements the first two terms of the control law, and a proportional controller K_p (28) implements the flywheel angular velocity feedback. A $r_\omega(t)$ reference for this velocity can be also added, as shown in Fig. 9.

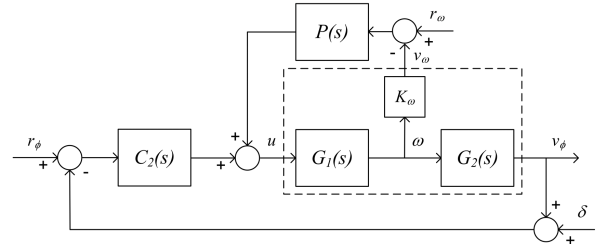


Figure 9: State feedback based FIP control loop

$$C_2(s) = \frac{K_{sf1} + K_{sf2}s}{K_m} = K_{c2} (1 + T_{d2}s) \quad (27)$$

$$K_p = \frac{K_{sf3}}{K_\omega} \quad (28)$$

These parameters are calculated from K_{sf} giving $K_{c2} = 21.3$, $T_{d2} = 0.21$ and $K_p = 2.31$, considering a flywheel angular velocity sensor gain given by $K_\omega = \frac{1}{30} [Vs/rad]$.

The system responses are plotted in Fig. 10, for the same initial condition and measurement disturbance applied to the PID with filter control strategy shown in Fig. 6. Now, the closed loop is internally stable, as there is no pole/zero cancellation at the origin, so r_ϕ is kept constant. Also, a steady-state error in the flywheel angular velocity $v_{\omega\infty} \approx 1.25$ is obtained in response to a step change $r_\omega(t) = 2.5$ at $t=2.5[s]$, applied to stabilize the pendulum with less energy. An augmented system with an error integrator should be arranged to avoid this steady-state error.

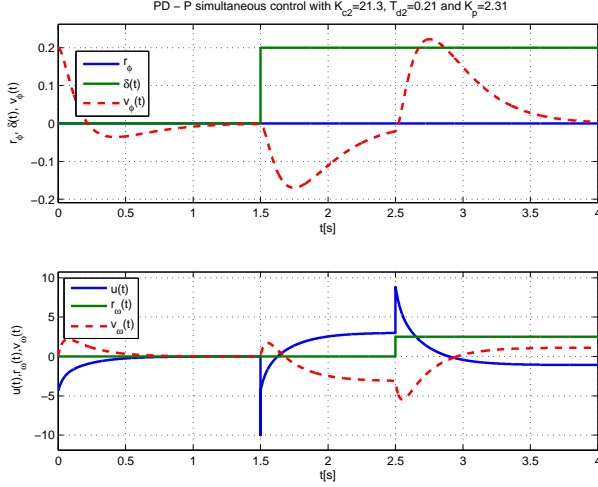


Figure 10: State feedback based control: Time responses

4.3. Observer-based output feedback stabilizing controller

The previous solution requires an extra sensor for the flywheel angular velocity, in addition to the pendulum position sensor and a PD controller, which will amplify the measurement noise, if any. If only the output is measured and the derivative noise is not acceptable, an observer can be designed to estimate the full state, as one of the advantages of the state observer is its filtering properties.

4.4. Experimental results

The control strategy shown in Fig. 4 has been implemented with the laboratory prototype [7]. The experimental results are summarized in the following figures. In Fig. 11, the inverted pendulum angular position is initially controlled with the manufacturer internal PID analogue controller, showing high frequency oscillations in the control action and the output signals. The manufacturer analogue PID control based strategy introduces strong ripple in the control action due to the continuous changes made around the setpoint to deal with the internal instability.

At $t=25[s]$, the pendulum is stabilized in the upper position with the proposed PID plus filter control strategy. Then, at $t=42[s]$, a change in the control input reference $r_u(t)$ is introduced, and 3[s] later the equilibrium position is recovered, with minor disturbances, although a small chattering appears in steady-state. Then at $t=63[s]$, the internal analogue PID control is restored. In the same experiment, the evolution of the control

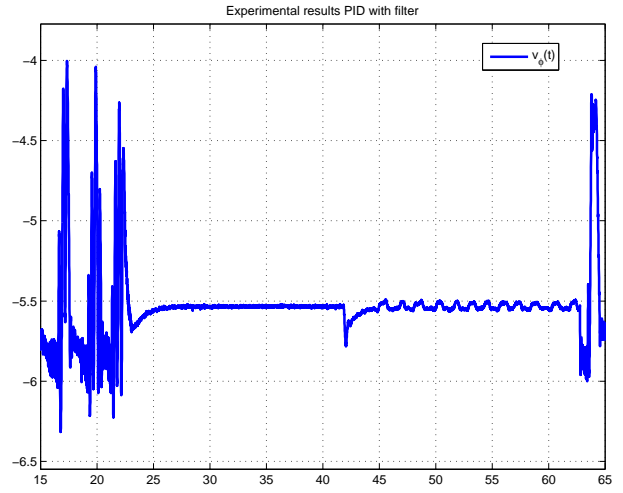


Figure 11: Experimental filtered PID FIP position control

action is plotted in Fig. 12. At $t = 42[s]$ the control input reference $r_u(t)$ has been changed to get the pendulum stabilized with minimum energy.

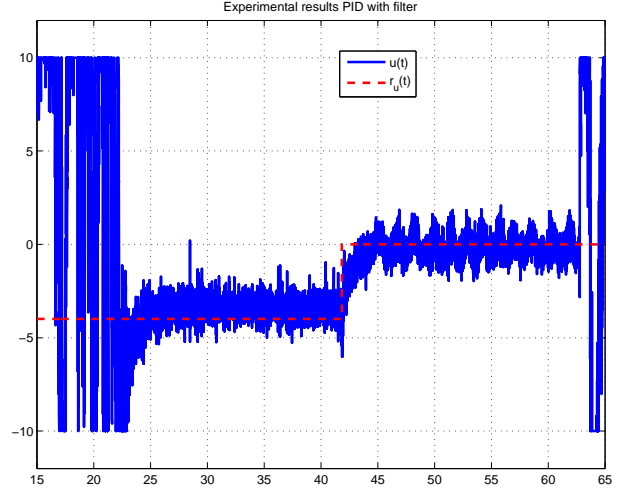


Figure 12: Experimental filtered PID FIP control action

5. Conclusions

An underactuated system, the so-called flywheel inverted pendulum, has been studied and a simplified model has been derived. The parameters of the experimental rig, available at the laboratory, allow to get a numerical model used to analyze the structure of the plant, as well as to design linear controllers.

The control structure is developed in two steps. First an output stabilizer PID controller is obtained following a traditional control design. The appearance of internal instability demands for a second control loop, which has been also designed by a simple control design method.

This strategy has succeeded to meet two simultaneous objectives with only one control action. That is, the stabilization of

the pendulum in the unstable vertical position, with compensation of small measurement disturbances, allowing the user to set the flywheel angular velocity to achieve such stability with minimum energy.

An alternative control structure could be implemented, based on a state feedback controller, avoiding the pole/zero cancellation problem leading to the internal instability, but it has not been implemented because no flywheel angular velocity sensor is available yet. This is a matter of further design (using an observer) and experimentation.

Further refinements in the control structure and implementation are sought to reduce the noise in the control action. The steady-state chattering seems to be unavoidable, up to now, when the pendulum position is controlled with zero flywheel angular velocity, due to nonlinearities such as the dead zone present in that operating region. Also, the steady-state error in the control action - flywheel angular velocity will be analyzed.

Acknowledgment

The authors want to thank the Universidad Técnica Federico Santa María providing a grant to Prof. Albertos as a research visitor.

References

- [1] M. W. Spong, *Underactuated Mechanical Systems, Control Problems in Robotics and Automation*, Springer-Verlag, 1997.
- [2] I. Fantoni, R. Lozano, *Non-Linear Control for Underactuated Mechanical Systems*, Springer-Verlag, 2002.

- [3] J.-J. Wang, Stabilization and tracking control of x-z inverted pendulum with sliding-mode control, *ISA Transactions* 51 (2012) 763–770.
- [4] F. Gomez-Estern, R. Ortega, F. Rubio, J. Aracil, Stabilization of a class of underactuated mechanical systems via total energy shaping, in: 40th IEEE Conference on Decision and Control, Orlando, FL, USA, 2001.
- [5] M. Bettayeb, C. Boussalem, R. Mansouri, U. Al-Saggaf, Stabilization of an inverted pendulum-cart system by fractional pi-state feedback, *ISA Transactions* 52 (2013) doi:<http://dx.doi.org/10.1016/j.isatra.2013.11.014>.
- [6] M. Olivares, P. Albertos, On the linear control of underactuated systems: the flywheel inverted pendulum, in: 10th IEEE International Conference on Control & Automation (ICCA 2013), Hangzhou, China, 2013.
- [7] E. D. Technologies, *Operating Manual of the Inverted Pendulum System*, model IP-NC (2002).
- [8] H. Yu, Y. Liu, T. Yang, Tracking control of a pendulum-driven cart-pole underactuated system, in: *IEEE International Conference on Systems, Man and Cybernetics (SMC'2007)*, Montreal, QC, Canada, 2007.
- [9] R. Ortega, M. W. Spong, F. Gomez-Estern, G. Blankenstein, Stabilization of a class of underactuated mechanical systems via interconnection and damping assignment, *IEEE Transactions on Automatic Control* 47-8 (2002) 1218–1233.
- [10] A. Shiriaev, A. Pogromsky, H. Ludvigsen, O. Egeland, On global properties of passivity-based control of an inverted pendulum, *International Journal of Robust and Nonlinear Control* 10 (2000) 283–300.
- [11] R. Kelly, R. Campa, Control basado en IDA-PBC del péndulo con rueda inercial: Análisis en formulación Lagrangiana, *Revista Iberoamericana de Automática e Informática Industrial (RIAI)* 2 (2005) 36–42.
- [12] M. W. Spong, P. Corke, R. Lozano, Nonlinear control of the reaction wheel pendulum, *Automatica* 37 (2001) 1845–1851.
- [13] X. Ruan, Y. Wang, The modelling and control of flywheel inverted pendulum system, in: 3rd IEEE International Conference on Computer Science and Information Technology, Chengdu, China, 2010.
- [14] D. J. Block, K. J. Aström, M. W. Spong, *The Reaction Wheel Pendulum*, Vol. 1 of *Synthesis Lectures on Control and Mechatronics*, Morgan & Claypool, 2007.